Accepted Manuscript

Characterisation Methods for Powder Bed Fusion Processed Surface Topography

S. Lou, X. Jiang, W. Sun, W. Zeng, L. Pagani, P.J. Scott

PII:	S0141-6359(18)30034-5
DOI:	10.1016/j.precisioneng.2018.09.007
Reference:	PRE 6839
To appear in:	*Precision Engineering*
Received Date:	16 January 2018
Accepted Date:	18 September 2018

Please cite this article as: S. Lou, X. Jiang, W. Sun, W. Zeng, L. Pagani, P.J. Scott, Characterisation Methods for Powder Bed Fusion Processed Surface Topography, *Precision Engineering* (2018), doi: 10.1016/j.precisioneng.2018.09.007

Characterisation Methods for Powder Bed Fusion Processed Surface Topography

S. Lou[1], X. Jiang[1*], W. Sun[2], W. Zeng[1], L. Pagani[1], P. J. Scott[1]

[1] EPSRC Future Metrology Hub, University of Huddersfield, Queensgate, Huddersfield, HD1 3DH, UK

[2] National Physical Laboratory, Engineering, Materials and Electrical Science, Hampton Road, Teddington, Middlesex, TW11 0LW, UK

* Corresponding author x.jiang@hud.ac.uk

Abstract

Powder bed fusion (PBF) is a popular additive manufacturing (AM) process with wide applications in key industrial sectors, including aerospace, automotive, healthcare, defence. However, a deficiency of PBF is its low quality of surface finish. A number of PBF process variables and other factors (e.g. powders, recoater) can influence the surface quality. It is of significant importance to measure and characterise PBF surfaces for the benefits of process optimisation, product performance evaluation and also product design. A state-of-the-art review is given to summarise the current research work on the characterisation of AM surfaces, particularly PBF surfaces. It is recognised that AM processes are different from conventional manufacturing processes and their produced surface topographies are different as well. In this paper, the surface characterisation framework is updated to reflect the unique characteristics of PBF processes. The surface spatial wavelength components and other process signature features are described and their production mechanisms are elaborated. A bespoke surface characterisation procedure is developed based on the updated framework. The robust Gaussian regression filter and the morphological filters are proposed to be used for the separation of the waviness component due to their robustness. The watershed segmentation is enhanced to extract globules from the residual surface. Two AM components produced by electron beam melting (EBM) and selective laser melting (SLM), are measured and characterised by the proposed methodology. Both of the two filters are qualified for the extraction of melted tracks. The watershed segmentation can enable the extraction of globules. The standard surface texture parameters of different surface wavelength components are compared. A set of bespoke parameters are intentionally developed to offer a quantitative evaluation of the globules.

Keywords

Surface texture; surface characterisation; additive manufacturing; powder bed fusion

1. Introduction

Moving from a rapid prototyping technique to a mature manufacturing technology, additive manufacturing (AM) is paving its way toward the next industrial revolution and has the potential to change the paradigm for manufacturing [1, 2]. By building products through the selective addition of materials in layers, AM offers a number of advantages over conventional subtractive manufacturing techniques, including reduced material waste, lower energy consumption and construction of geometrical structures not possible with traditional manufacturing processes [3]. As a powerful technology, AM impacts a multitude of key industrial sectors, such as aerospace, automotive, healthcare, defence and electronics. New industrial trends like bionics, light-weight construction or ‘mass customisation’ are all potential fields of application for AM.

Among various AM processes that are commercially available, Power bed fusion (PBF) is probably the most generic and popular technique that is directly used in the production of metal AM parts [1]. In PBF process, the thermal energy, e.g. laser or electron beam, selectively melts and fuses the specific region of a powder bed to create a solid structure. In comparison to other AM processes, PBF enables a large range of material options, including polymers, metals, ceramics and composites. In general, PBF is suitable for the production of parts with small-to-medium size,

low volume and complex geometries [4]. In aerospace and biomedical applications, metal PBF processes are increasingly used due to their capability to handle complex geometries and excellent material properties when compared to traditional metal manufacturing techniques [4]. Selective Laser Melting (SLM) and Electron Beam Melting (EBM) are the two common types of PBF processes.

In spite of the popularity and many advantages, the application of PBF is still limited by some major drawbacks such as low surface quality [5]. The surface finish of a part is critical in many applications, e.g. aerospace, healthcare. In some applications, a surface roughness of Ra 0.8 μm or better is required to avoid premature failure from surface initiated cracking [6]. Even for consumer products, AM parts have common surface textures that may need to be modified for aesthetic or performance reasons. To overcome this problem, post processes are usually required to improve surface finish. A variety of surface modification technologies are available for this purpose, comprising mechanical processes (machining and abrasive sandblasting), chemical processes (acid etching and oxidation) and thermal processes (plasma spray). However, these additional processes not only incur further time and cost, but also delay part completion, compromising the advantages of using AM processes for industrial production.

The PBF process variables have direct impacts on the generated part surfaces. Among the full set of PBF process variables, three variables, i.e. energy density, building orientation and layer thickness, have been identified to have significant influences on surface topography. Mumtaz and Hopkinson [7] found that in SLM processes high laser peak power tended to reduce both top and side surface roughness as recoil pressures flatten out the melt pool and reduce balling formation; increasing laser repetition rate and reducing scan speed reduced top roughness but increased side roughness. It was observed that the AM surface topography also varies with building orientation angle [8]. Surface topography of the horizontal surface (0°) is dominated by the ripple effect; as the inclination angle gradually increases, the stair-case effect (i.e. the stepped approximation by layers of curves and included surfaces) then starts to take the key role, showing as obvious waves on the surface. For surfaces with inclination angles greater than 45°, the isolated peaks (caused by incompletely melted particles) will become the dominant feature. The research work of Ghanekar [9] showed that decreasing layer thickness can reduce the so-called staircase effect and therefore the surface roughness. Bacchewar *et al.* [10] found that for upward-facing surfaces, building orientation and layer thickness were significant parameters; for downward-facing surfaces, other than build orientation and layer thickness, laser power was also an important factor. There are more process variables than those aforementioned which can influence AM surface topography. Changing of the hatching distance (the distance between neighbour scanning vectors) can cause modification in geometric characters of melted tracks and consequently surface topography [11]. Gravity can affect melt pools that are created on the unsupported layers. Gravity causes melt pools to sag into the un-melted powder bed below, resulting in a much rougher surface on the underside of the component than on the upward facing surfaces [12]. Scan pattern tends to produce multidirectional texture underlying lay and laser path changes can cause the part to distort in certain directions than others.

Apart from AM process variables, a few other factors may also affect the surface topography of produced AM components. The shape, size and spreading of material powder strongly influence laser absorption characters, and thus influence the produced surface. For example, the finer the powder particles are, the smoother the produced surface is. However, finer powders are normally more difficult to spread and handle and they also increase the opportunity that the unmelted particles stick to the surface [13]. In contrast, larger powder particles are easier to handle and spread, but they limit surface finish, minimum feature size and minimum layer thickness. The orientation of the parts to the recoater blade that spreads powder during the build, can also affect surface topography [12]. The motion of the recoater can damage the distorted layer surface caused by residual stress and it was found that the vertical surface and the downward facing surface can be discerned by the nature of damaged material [14]. The damaged material is scraped into the part from the vertical surface and out of the part from the downward-facing surface.

Measuring and characterising surface topography is critical for the product inspection and quality control. Furthermore, the advanced knowledge of surface topography will benefit AM product design. Designers can optimise products' geometry to minimise the post processing if the links between surface topography and AM process is well understood [15].

This paper aims to update the traditional surface characterisation framework to better fit into the AM context, based on which a bespoke procedure to characterise PBF processed surfaces is proposed. The paper is constructed in the following fashion. Section 2 presents the state-of-the-art summary of recent work on AM surface characterisation. In Section 3, an updated description of surface wavelength components and topographical features of PBF surfaces is presented. Subsequently, a procedure to characterise various PBF produced signature features is proposed. Section 4 details three techniques that are proposed for the extraction of waviness, roughness and globules/surface pores. Case studies of applying these characterisation techniques to SLM and EBM processed surfaces are illustrated in Section 5. Finally, Section 6 reaches a brief conclusion.

2. State-of-the-art summary of AM surface characterisation

The complex nature of AM processes tends to produce components with surfaces that have a roughness ranging from a few micrometres to several hundreds of micrometres and with versatile topographical features. The complex AM surface topography is challenging for existing surface characterisation methods.

2.1 Surface filtration and analysis

Surface filtration is the technique by which various spatial wavelength components of the surface texture, namely roughness, waviness and form error, are extracted from the measured data for further characterization [16]. A variety of filtration techniques, including the Gaussian filter, the Spline filter, morphological filter etc. are available for the extraction of surface wavelength components. Among these, the Gaussian filter is widely accepted and regarded as the standard filtration method for surface texture filtration. Recent published research work that involves the use of the Gaussian filter for AM produced surfaces follows the standard surface characterisation procedure, i.e. the Gaussian filter is first applied to separate the roughness component followed by the quantisation of roughness parameters. Nonetheless, the variety of selected cut-off wavelengths is noticed. Grimm *et al.* [17] used the cut-off λ_f 5 mm to supress the form error component and λ_c 1 mm to supress the short wavelength component of SLM surfaces. Fox *et al*. [14] took λ_s 0.025 mm and λ_c 0.8 mm for the filtration of DMLS surfaces and an evaluation length equal to five λ_c cut-off wavelengths, i.e. 4 mm. Vetterli *et al.* [18] employed different surface measurement instruments to measure Selective Laser Sintering (SLS) surfaces and followed λ_c cut-off wavelengths recommended by each individual instrument, e.g. 0.8 mm, 1.1 mm and 2 mm. They also investigate the influence of cut-off wavelength on roughness evaluation. Triantaphyllou *et al.* [12] used the areal scale fractal analysis to examine the complexity of both SLM and EBM surfaces and deduced that λ_c 2.5 mm appears sufficient to capture the data required to characterise AM surfaces. The question in selecting cut-off wavelengths is that it is not clear what roughness and waviness mean to AM processes and it is unsure whether current relevant ISO standards apply to AM surface texture. It was also noticed that in these literatures (except [17]) the waviness has rarely been studied. Nonetheless the characterisation of the waviness is of necessity from both process control and performance evaluation points of view.

The common use of filtration techniques to separate surface wavelength components can partially indicate the surface quality of additive processes. However, if surface topography is to be used as a process signature, the conventional method to separate surface wavelength components is not adequate. Instead, a strong quantitative understanding of the relationship between the mechanisms that contribute to surface texture and measured surface parameters must be understood [14]. Thus, the filtration techniques should not be simply applied to separate waviness and roughness of the AM surfaces as they are commonly used for traditionally machined surfaces,

but ought to contribute to relating surface topography with AM processes. This critical fact is recently recognised by a few researchers and some initial research work has been conducted. Reese *et al.* [19] proposed to create a richer language to describe "as printed" AM surfaces and eventually aimed to relate to the process parameters to the surface topography of the final part. They also proposed to use the power spectrum density to investigate the scan/step frequency and the watershed segmentation method [20] to analyse the hills and pits on AM surfaces. Senin *et al.* [21] developed a series of image processing techniques for the extraction and analysis of the topographical features of PBF surfaces. Lou *et al.* [22] developed an enhanced watershed segmentation method to extract the incompletely melted powder particles from SLM surfaces. A similar work was presented by Rosa et al. [23] where the partially melted particles were extracted from Directed Metal Deposition (DMD) processed surfaces using a thresholding method.

2.2 Surface parameterisation

Following surface filtration, surface parameterisation provides a quantitative evaluation of surface texture. ISO 4287 [24] defined the profile surface texture parameters, e.g.Ra, Rq, Rsk, Rku while a whole family of areal surface texture is given by ISO 25178-2 [20], such as Sa, Sq, Ssk, Sku. For industry manufacturers, they tend to use the profile parameter Ra and Rq or their areal counterpart Sa and Sq to evaluate AM surface finish. However, the use of these surface texture averaged height parameters can only reveal a limited amount of information that may restrict the benefits of surface metrology for AM process controlling. Fox et al. [14] claimed that Ra can only provide little insight into characters of DMLS surfaces while other parameters are more meaningful. For example, Rc increases and RSm decreases as surfaces change from being dominated by the re-solidified melt tracks to being dominated by the partially melted powder particles.

Areal surface texture parameters were found to be more useful than their profile counterparts. Sidambe [25] investigated the surface topography of EBM produced surfaces in terms of three building angles, i.e, 0°, 55°, 90° and found Sa, and Sq show a much better correlation to the building angle than Ra and Rq. His work also showed that the 0° and 90° surface have negative Ssk values while the 55° surface has a positive Ssk. He explained that the 0° surface and the 90° surface have squashed texture predominated by valleys whereas the 55° surface has relative small edge radius and is predominated by peaks. Ssk was also found to be able to differentiate the upskin from the downskin of both as-built and post-processed SLM coupons [12]. The surface of SLM parts showed quite strong correlation between surface orientation and the areal parameters Str and Sdq [17]. The scan/step frequency was found to increase monotonically with the angle of the build [19]. The investigation of Lemoine et al. [26] showed that multi-scale fractal parameters correlate well with the linear energy density of SLM process.

Apart from using traditional profile and areal surface texture parameters, there are also recent attempts on developing new parameters for AM surfaces. Lou et al. [22] designed a set of parameters to quantify the unmelted/partially melted particle clusters on PBF surfaces. Rosa et al. [23] proposed the parameters to indicate the density of particles and related these parameters to the DMD process parameters, particularly the laser power and the mass feed rate. Similarly, Senin et al. [21] presented the characterisation of spatter features and weld tracks on PBF surfaces. Pagani et al. proposed an extension of the definition of the areal texture parameters to any generic freeform surface, which are very suitable to describe AM manufactured surfaces with non-planar geometry, including re-entrant features [27].

Investigating traditional surface texture parameters and new bespoke parameters for AM surface texture characterisation are both necessary for linking AM surface texture with AM processes and AM product functionality. However, more systematic and experimental research is required for the validation and verification of these parameters.

3. Proposed methodology for surface characterisation of PBF surfaces

3.1 An updated description of surface wavelength components and topographical features of PBF surfaces

Surface metrology originated from the need to control manufacturing since the surface geometry of the part being made was extremely sensitive to changes in both process and machine tool performance [28]. Measured surfaces with form removed can be decomposed by filtration techniques into three spatial wavelength components, i.e. roughness, waviness and form error, such that the characterisation of these various wavelength components can provide an indication of corresponding machining faults [29].

The existing surface characterisation framework was mainly developed for traditional manufacturing technologies. As a consequence of manufacturing changes, especially the emergence of AM as a mature manufacturing technology, this framework needs to be updated and reflect AM's unique characteristics. AM parts have an unusual surface topography which is not comparable to conventionally machined surfaces. Existing surface characterisation methods are not directly applicable to AM surfaces. Particularly it should be addressed that AM processes differ from traditional machining techniques (e.g. turning, milling, polishing) and this critical fact should be taken into account when characterising AM surface topography, which is often unconsciously neglected. AM process features complex physical interaction that occurs during melting and solidification of materials. Various topographical features are presented on AM surfaces as the signatures of its manufacturing process. The surface characterisation framework should be updated to reflect the characters of AM processes.

Figure 1 illustrates typical surface topography of PBF components. The immediately recognisable surface topographical features include stair-steps, powder adhesion and surface pores. Stair-stepping is a fundamental issue in all layered manufacturing, although one can choose a thin layer thickness to minimise error at the expense of build time. Powder adhesion is a fundamental characteristic of PBF processes. The amount of powder adhesion can be controlled, to some degree, by changing part orientation, powder morphology and thermal control technique [4]. Surface pores appear as small recesses, sometimes showing portions of the layer underneath [29]. All these features are closely linked to the AM process. Thus, surface components defined in the conventional surface texture characterisation framework should be updated to reflect these characteristics. The description of roughness, waviness and form error of PBF processed surfaces is listed in Table 1. In addition, other topographical features that do not fall into the category of traditional surface wavelength components should also be clearly defined. Table 1 also presents the mechanisms that produce these surface components and topographical features. A notable phenomenon is that the surface topography of PBF may change in respect to its process variables. For example, as the building angle increases, the surface topography is changing from melted tracks dominated to incompletely particle dominated.

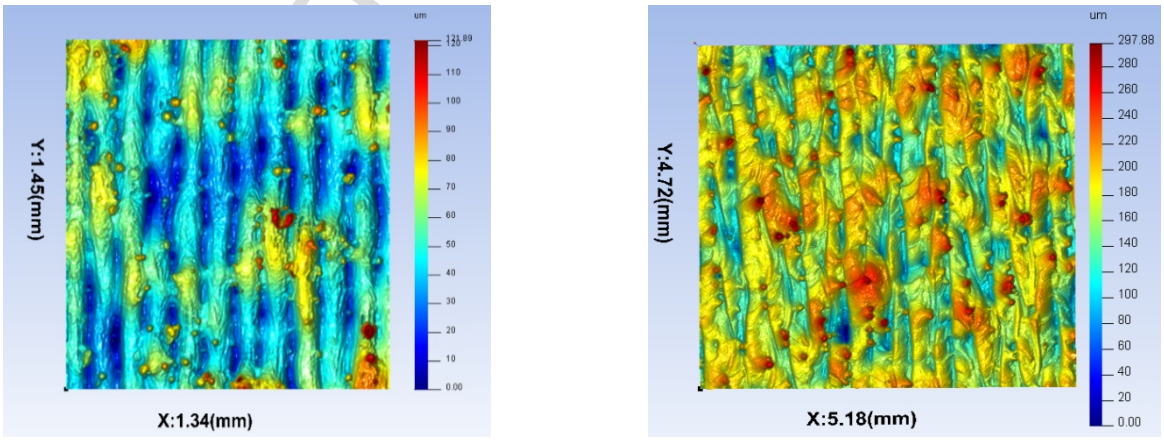

(a) (b)

Figure 1. PBF surface topography measured by optical focus variation technique. (a) an SLM surface; (b) an EBM surface.

Table 1. Description of surface topographical features of PBF surfaces and corresponding production mechanism.

Surface component	Description	Production mechanism
Roughness	Surface asperity in micro scale	Generated by the physical interaction between the laser beam/electron beam melting process and metal powder particles.
Waviness	Wave-like features reflecting the shape of the melted tracks	Formed by the Marangoni flow of melted metal liquid [30].
Form error	Shape distortion	Mainly caused by thermal effect [4].
Globules	Spherical protrusion features in various sizes	They can be either small size unmelted/partial melted particles adhered to the underlying surface, or medium size spatters originated from the metal liquid ejection due to melted pool overheat [31].
Surface pores	Small cavities in various sizes.	Either insufficient power or overheat of the melted poor [32, 33].

ISO 25178-2 [20] and ISO 25178-3 [34] have embodied the scale-limited surface which no longer requires defining surface texture parameters for three different categories as defined in ISO 4287 [35], i.e. P-parameters for the primary profile, R-parameters for the roughness profile and W-parameters for the waviness profile. These areal surface texture standards use S-filter, L-filter and nesting index for the generalised use of filtration techniques. While many professional metrologists and researchers within surface metrology have accepted these concepts, the conventional naming of surface texture characterisation is kept in this work for the benefits of the wider readers outside surface metrology area, particularly those in manufacturing industry.

3.2 Proposed surface characterisation procedure for PBF surfaces

PBF surface topography consists of not only the traditional surface wavelength components, i.e. roughness, waviness and form error, but also other signature features generated by PBF, such as globules and surface pores. The challenge in characterising PBF surface topography lies in the overlapping effect of these different features. The use of filtration techniques to extract waviness and roughness components should take the impact of all these significant signature features into consideration [36].

The proposed procedure to characterise process surfaces is in the following sequence. First surface waviness is extracted by using advanced filtration techniques. The robust Gaussian regression filter is a good candidate because it incorporates robust statistical estimation that can provide insensitivity against globules and surface pores. Alternatives are morphological filters. By choosing suitable morphological operations, it can either suppress steep peaks (i.e. globules) or sharp valleys (i.e. surface pores), or both at the same time. Both these two advanced filters do not require form removal. The residual surface is obtained as the surface that remains when the waviness surface is excluded. On this residual surface, the segmentation technique is employed to extract out globules and surface pores. These two different features can be identified according to their geometry, either convexity or concavity. The roughness component is taken as the surface portion obtained by excluding the globules and surface pores, and is used to provide the data reference from which the roughness parameters will be calculated.

4. Surface characterisation techniques for PBF surfaces

In this section, the surface characterisation techniques used for the analysis of PBF surface texture are detailed. The robust Gaussian regression filter and the morphological filters will be employed to extract melted tracks. The watershed segmentation will be used and enhanced to identify the

globules. All these characterisation techniques use the algorithms developed and implemented by the authors from the University of Huddersfield [37-39].

4.1 Extraction of waviness

The extraction of waviness is via the filtration techniques. However, the globules and surface pores can impede the application of the standard Gaussian filter, which is unable to handle outliers [37]. Instead, the use of advanced filtration techniques, including the robust Gaussian regression filter and the morphological filters, is proposed.

4.1.1 Use of the robust Gaussian regression filter

By incorporating the robust statistical estimators into the filtration process, e.g. the Tukey estimator, the robust Gaussian filter provides the robustness against specific phenomena in the input data, e.g. outliers, scratches and steps [40, 41]. For PBF surfaces, the globules and surface pores are regarded as the "outliers" since they feature significant high or low values compared to the surrounding data. Other merits of this filter are: it overcomes the running-in and running-out distortion of the standard Gaussian filter and it does not require surface form removal since the polynomial fitting is incorporated into the filtration [42].

For the convenience of visualisation, the comparison of the standard Gaussian filter and the robust Gaussian regression filter is conducted on the profile data which is extracted out from a measured EBM areal surface. Figure 2 illustrates such an example profile on which two significant signature features of the EBM process are observed. First, the EBM profile presents significant periodic waves, which are formed by melted tracks. Second, two large protrusions reside on top of the waves, which are the cross-section profiles of two globules. The profile data is used for the convenience of verifying the robustness against the globules. The λ_c and λ_f cut-off wavelengths are set to 0.25 mm and 4 mm respectively.

The waviness (reference) profiles generated by the standard Gaussian filter and the robust Gaussian regression filter are both shown in Figure 2(a). As highlighted by the red annotation in Figure 2(a), the reference profile resulted from the standard Gaussian filter intersects the globule feature in the middle, which subsequently shortens the amplitude of globule features on the residual profile, see Figure 2(b). It is also noticed that the standard Gaussian filter generated an expanded reference profile on the two sides of the globule feature due to its "mean-line" characteristic, i.e. it leads to equal areas below and above the reference profile. This effect, however, is undesired, because fake dimples are produced on the residual profile, marked by two blue annotations in Figure 2(b). These fake dimples will distort the extraction of globules. In comparison, the reference profile produced by the robust Gaussian regression filter runs right below the globule feature and the filter does not generate significant fake dimples in the residual profile.

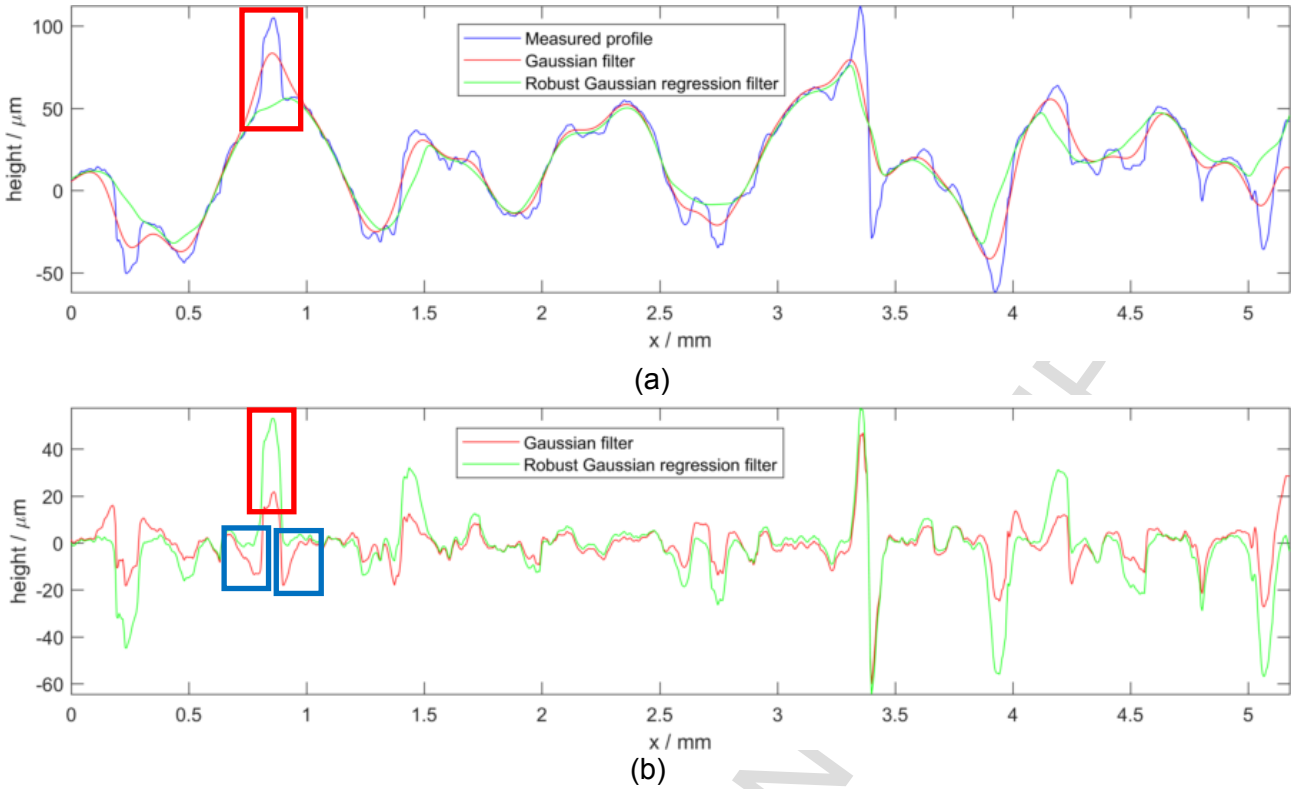

Figure 2. Extraction of waviness from an EBM surface profile using the robust Gaussian regression filter with λ_c 0.25 mm and λ_f 4 mm: (a) waviness profiles; (b) residual profiles.

4.1.2 Use of the morphological filters

Alternative techniques to suppress the impact of globules and surface pores on waviness extraction are morphological filters [43], which are more relevant to the functional evaluation of surfaces, e.g. assembly, sealing, contact phenomenon [44-46]. For the purpose of surface filtration, circular disks are commonly used for profile data, while spherical balls are used for areal data. The traditional algorithm of morphological filters is based on image processing, while advanced algorithms built on computational geometry are available, having better computational performance, no boundary distortion and being capable of using arbitrary size of disk/ball [38].

Two basic variations of morphological filters are the closing filter and the opening filter, which are upper and lower envelopes of moving balls. The probing of the workpiece surface using a tactile probe with a specified diameter is actually a hardware implementation of morphological closing operation. Depending on disk/ball radius, morphological filters can extract surface geometry in different scales: a large disk/ball results the large-scale geometry, e.g. surface form; a medium disk/ball generates the medium-scale geometry, e.g. waviness; and a small disk/ball reveals the fine-scale geometry.

To apply morphological filters to PBF surfaces, two considerations should be placed to ensure a proper selection of disks/balls: (1) the disk/ball can extract the waviness, i.e. the wavy shape of melted tracks; and (2) they can suppress the impact of globules or surface pores. Two examples of applying the opening filter and the closing filter are presented in Figure 3 and Figure 4 respectively. Figure 3(a) presents the application of the opening filter on the EBM profile previously used in Figure 2. The disk radius is set to 0.25 mm. As Figure 3 illustrates, the opening envelope can reveal the wavy shape of melted tracks. Meanwhile, two sharp globule peaks whose curvatures are smaller than the used disk are suppressed. Since the opening envelope is the rigorous lower boundary, topographical features on the residual profile are all peaks, see Figure 3(b). Nonetheless, the two globule peaks are dominant, while other peaks are less significant. This can benefit the subsequent globule segmentation. In Figure 4(a), the closing filter with a disk of radius

0.1 mm is applied to a measured SLM surface profile, where a significant surface pore is presented. Because the closing filter generates a rigorous upper boundary, it suppresses the sharp valleys whose curvatures are smaller than that of the disk. The residual profile is flattened by the closing filter and thus only contains valleys. This can facilitate the extraction of surface pores.

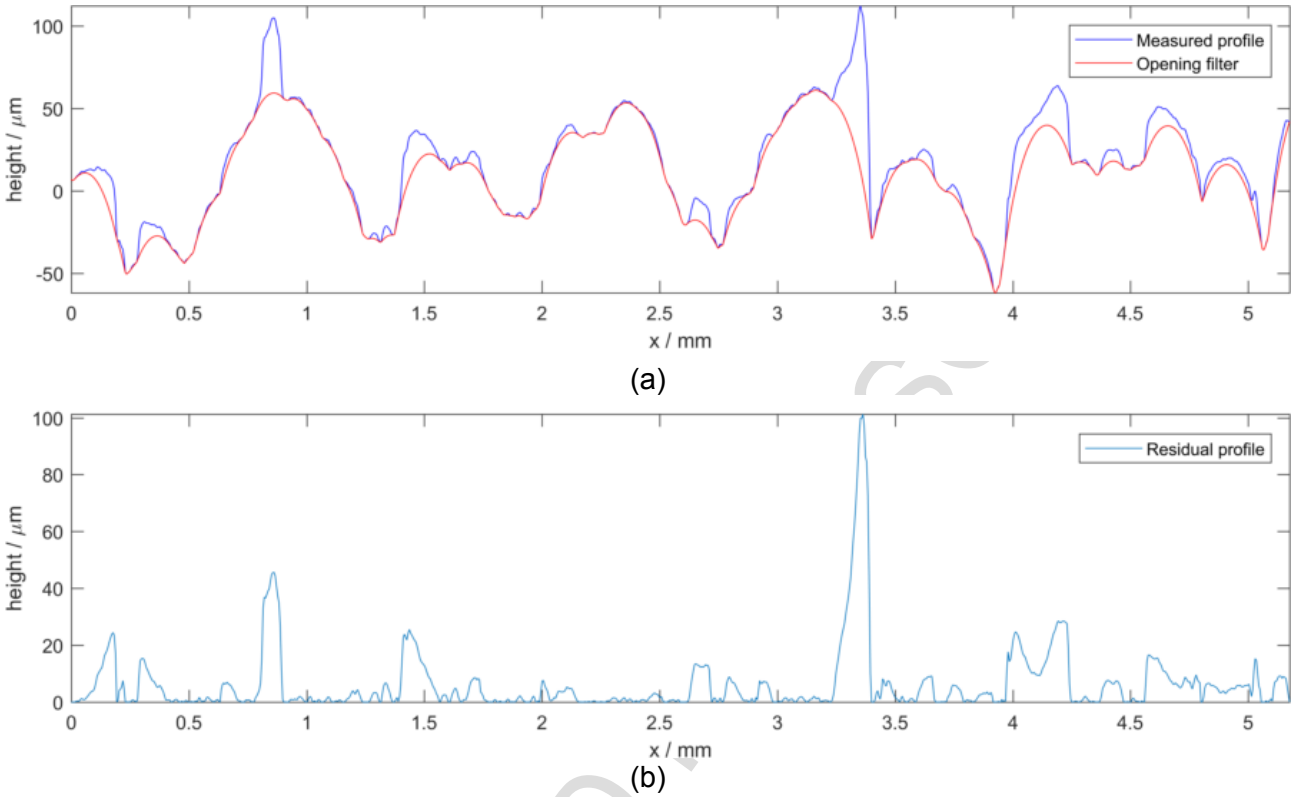

Figure 3. Extraction of waviness of an EBM surface profile using the morphological opening filter with a disk of radius 0.25 mm: (a) opening envelope; (b) residual profile.

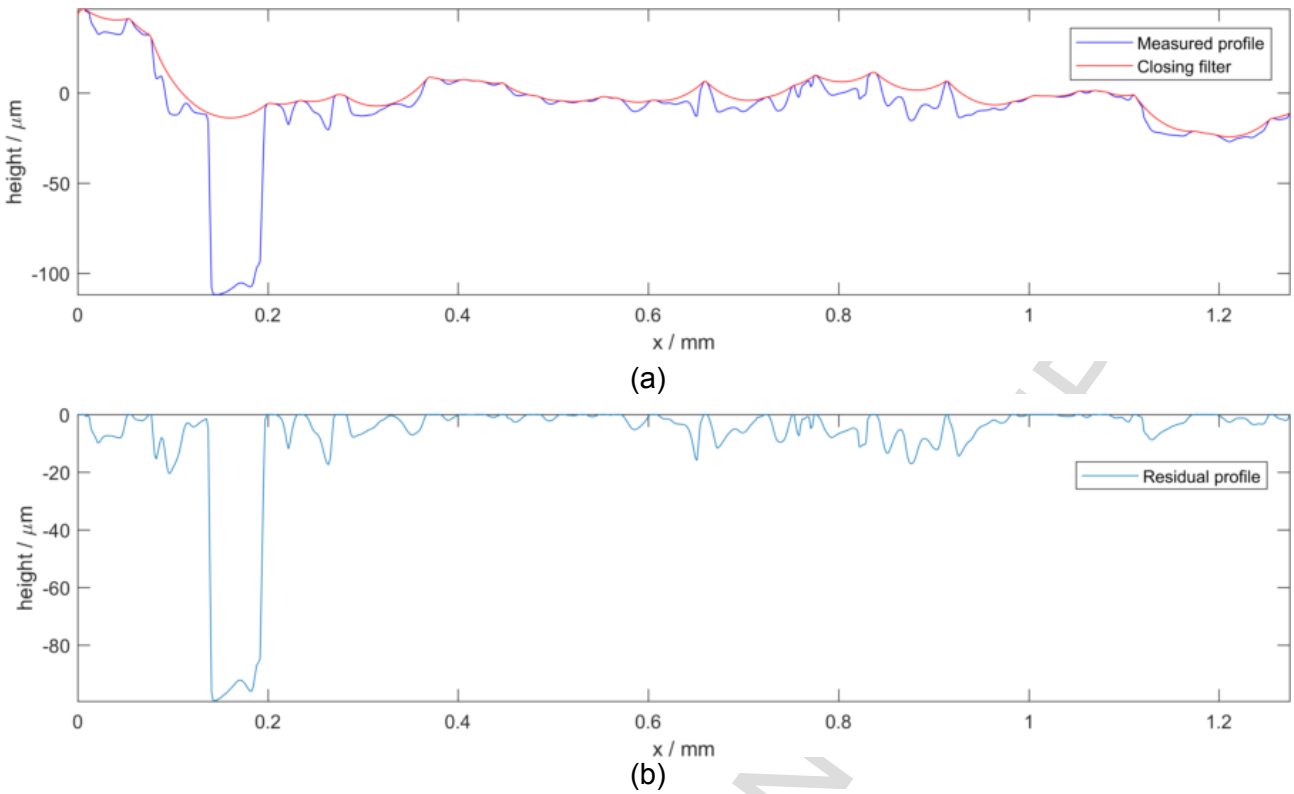

Figure 4. Extraction of waviness of an SLM surface profile using the morphological closing filter with a disk of radius 0.1 mm: (a) closing envelope; (b) residual profile.

The opening and closing filter can even be combined to achieve a compound effect, which is called the alternating symmetrical filter (ASF) if the same size of structuring element is used for both the two filters, the combined filter. Two ASF options are available, either closing followed by opening, or opening followed by closing. In both cases, ASF can suppress globules and surface pores in one run, achieving a similar effect to the robust Gaussian regression filter, see Figure 5. The type of ASF should be selected in response to the characteristics of the surface. If globules are dominant features, then the combination of “opening + closing” is more suitable, because the first morphological operation in the combination takes a stronger role. This is evidenced by Figure 5. If surface pores are the dominant feature, then the combination of “closing + opening” is opted. It should be noted that the sizes of disks/balls used in ASF do not have to be the same. In actual, their sizes can be determined according to the physical sizes of globules and surface pores. In this case, ASF becomes to the more generalised filter, the alternating sequential filter [47]. For example, if the size of globules is smaller than that of surface pores, then a small disk/ball should be used for the opening filter and a larger disk/ball for the closing filter.

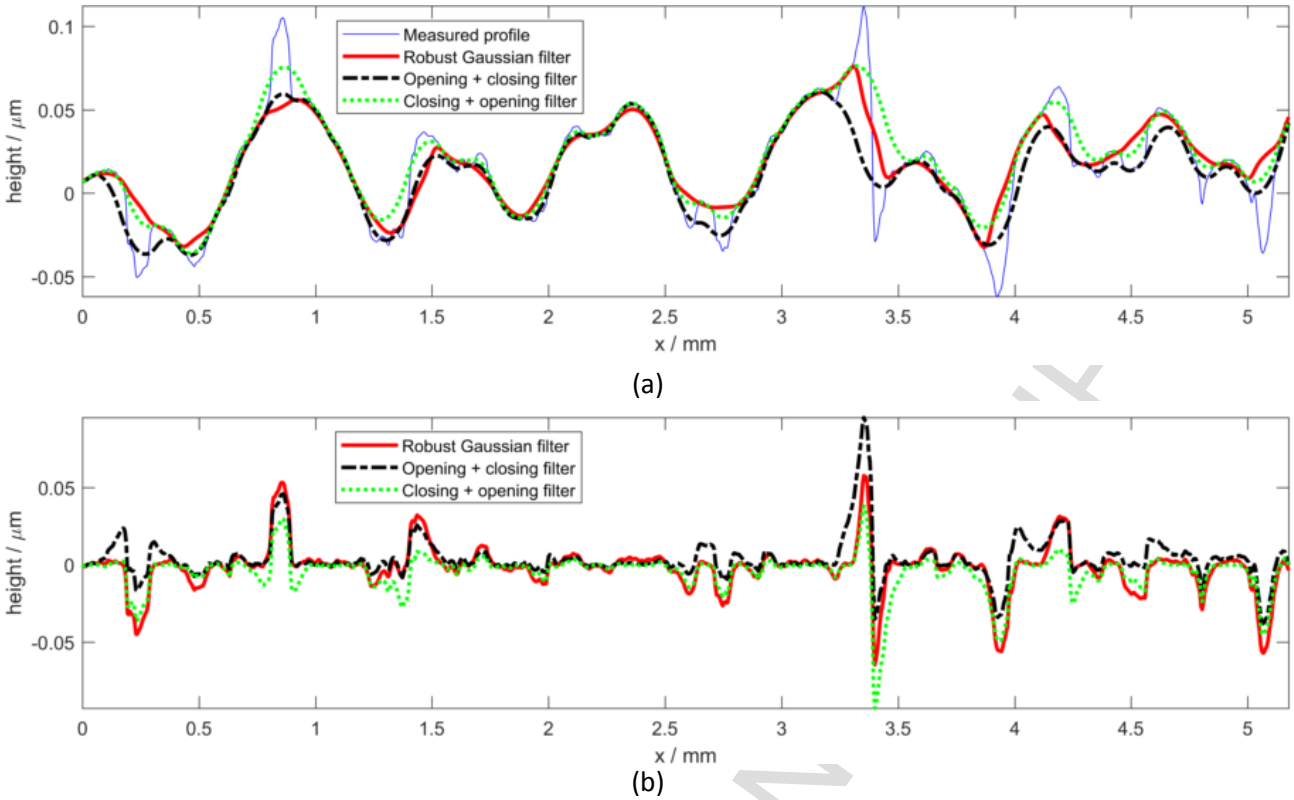

Figure 5. Extraction of waviness of an EBM surface profile using the robust Gaussian filter, the "opening + closing" ASF and the "closing + opening" ASF: (a) waviness profiles; (b) residual profiles.

4.2 Extraction of globules/surface pores by the watershed segmentation

In comparison to the surface wavelength components (i.e. roughness, waviness and form error) that span over the whole surface, globules and surface pores are isolated geometries and distribute almost randomly on AM surfaces. The watershed segmentation is employed to extract these isolated features.

The watershed segmentation, originated from geography, can partition a landscape into a number of small patches. Suppose a landscape is flooded by raining, the rainwater naturally flows down the steepest paths and eventually falls into a number of domains of attraction (called the catchment basins). The watersheds, being the dividing lines of these catchment basins, are the natural segmenting contours of the landscape. This method has been successfully employed to analyse topographical features on engineering surfaces, such as grinding wheels and car body panels [48]. The segmentation of PBF surfaces is more challenging in comparison to traditional engineering surfaces. As Table 1 lists, a diversity of signature features is presented on PBF surfaces due to different production mechanisms, and globules and surface pores reside on the underlying melted tracks. To enable a valid watershed segmentation of globules/surface pores, the melted track waves need to be suppressed by using the robust Gaussian regression filter or morphological filters as described previously.

The globules are steep hills on PBF surfaces featured by large gradients at their boundary and high surface amplitudes in comparison to the neighbouring surface. Edge enhancement is required to reinforce the feature boundary and enable the subsequent segmentation analysis to obtain a more representative extraction. This is achieved by first applying the Gaussian filtering with a short wavelength cut-off to suppress very high frequency measurement noise and to smooth topographical features followed by application of the Sobel operator [48] to yield a gradient map of the processed surface data. Figure 6(a) presents a small portion of the surface measured from an SLM component. Figure 6(b) shows the gradient map (gradient norm) of the surface. The

watershed segmentation is then applied to the gradient map, generating a sequence of small segments. Figure 6(c) presents the resulted segmentation contours spatially superimposed on the original measured surface. An issue raised by the watershed segmentation is that it tends to produce over-segmentation, i.e. tiny segments are often produced due to local trivial topographical features or measurement noises. However, it can be recognised that the boundary of those segments that contain partial boundaries of a globule can be jointed and merged to form an enclosed contour of that globule feature. Therefore, the segments belong to a certain globule are identified and combined to present a significant globule feature. To this purpose, the threshold of 36 μm is applied, which is three standard deviations above the mean height of the surface [22]. Those surface patches with their height above this threshold are extracted and merged. See Figure 6(d) for the extracted globules. The surface pores can be extracted in a similarly manner. The only difference is that they feature steep cavities and are presented as surface dales.

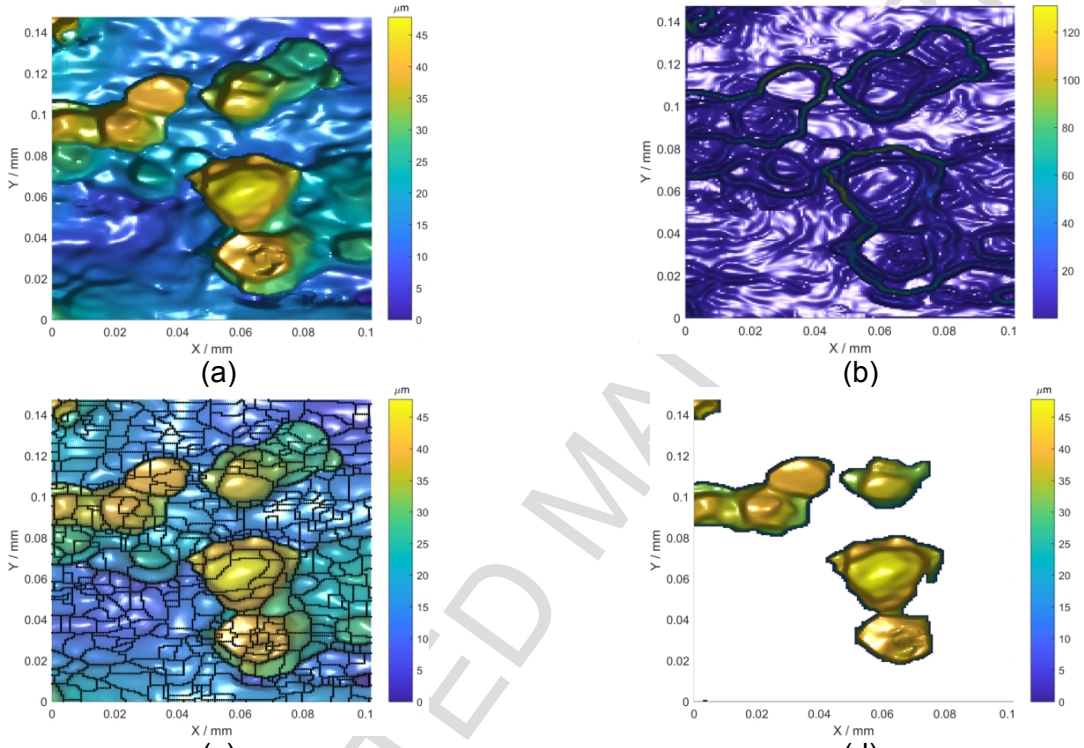

Figure 6. Extraction of globules using the watershed segmentation with the height threshold 36 μm: (a) original surface; (b) gradient map; (c) watershed segmentation; (d) extracted globules.

5. Case studies

5.1 EBM surfaces

A group of surface measurements were performed on an EBM component using the Alicona InfiniteFocus G4 system. The EBM surface was measured using the following configuration: 10x objective lens, ring light, vertical resolution 1.41 μm, lateral resolution 3.91 μm, sampling distance 5.22 μm (after data decimation), and 3x4 stitching. The measurements were conducted at six different sites uniformly over the surface. The procedures described in Section 3.2 are employed for surface characterisation.

Figure 7(a) presents the measured EBM surface with the size of 4.72 mm x 5.18 mm. Its surface topography is dominated by melted tracks. Globules are also seen sitting on melted track waves. The robust Gaussian regression filter is applied first to separate the waviness surface, see Figure 7(b). The λ_c cut-off wavelength is intentionally set to 0.25 mm, which can separate the smallest melted tracks. The λ_f cut-off wavelength is set to 4 mm to remove form error. The residual surface

is generated by subtracting the waviness surface from the original measured surface, see Figure 7(c). Following the waviness separation, the watershed segmentation with the height threshold 140 μm is then applied to extract the globules from the residual surface. Figure 7(d) and 7(e) illustrate the identified globules on the residual surface and the original measured surface respectively. Figure 7(f) presents the underlying roughness surface obtained by excluding the globules from the residual surface.

Table 2 lists four surface texture parameter results, i.e. Sa, Sq, Ssk, Sku, for three different surface wavelength components, i.e. the waviness surface, the residual surface and the roughness surface. Both the mean values and the standard deviations of the measurements are listed in the table. The comparison of these parameters between the residual surface and the roughness surface reveals the impact of globules on surface texture characterisation. It is noticed that the Sa and Sq of the residual surface are 3.5% and 9.3% higher than those of the underlying roughness surface due to the fact that the globules increase surface roughness. The Ssk parameters of both the residual surface and the roughness surface are negative values. This is because the valleys, i.e. the gaps between melted tracks, dominate the EBM surface topography. The globules contribute to the positive Ssk, and thus taking out the globules decreases Ssk. The values of Sku parameters of both the residual surface and the roughness surface are above 3. This implies that surface heights are not normal distributed but contain sharp features, e.g. globules. As the globules are excluded, the Sku parameter decreases because the underlying roughness surface is flatter. The parameterisation of globules of the EBM surface is given in Table 3, which consists of the total globule areas, the globule area percentage to the whole surface and the total globule volume. The volume parameters are calculated based on the residual surfaces, e.g. Figure 7(d) and Figure 8(d). This is because the waviness surfaces generated by the robust Gaussian filter and the morphological opening filter can be taken as the reference bases.

The alternative method to separate the waviness is the morphological opening filter. Figure 8(b) shows the opening envelope using a ball of radius 0.2 mm. The residual surface is shown in Figure 8(c). Because the opening envelope generates a rigorous lower boundary, the residual surface has a flatten base. The globules are then identified using the watershed segmentation with the height threshold of 80 μm, see Figure 8(d)-(f). The results of surface texture and globule parameters are listed in Tables 4 and 5 respectively. The comparison of the surface texture parameter results between the residual surface and the roughness surface is similar to that of the robust Gaussian regression filter.

By comparing the parameters results of the robust Gaussian regression filter and the morphological filters, it is found the Sa, Sq resulted from the robust Gaussian regression filter is larger than those generated by the opening filter, mainly because the waviness generated by the former filter is smaller in amplitude. This is also affected by the cut-off wavelength and the ball radius used by the filters. It should be noticed that there is not an equivalent relationship between the cut-off wavelength used by the Gaussian filter and the ball radius employed by the morphological filters. For instance, the Gaussian filtering using λ_c 0.2 mm does not imply morphological filtering with ball radius 0.2 mm. In this case, the criterion used in selecting the cut-off wavelength and ball radius is that these thresholds should enable a good extraction of the wavy shape of melted tracks. The Ssk, Sku results of the morphological opening filter are noticed to be higher than those of the robust Gaussian regression filter. The opening filter by its nature produces peaks on this residual surface and therefore the mean surface will shift towards peak portions. Its height distribution will be sharper than that of the robust Gaussian regression filter. The globule areas identified by the morphological filter are larger than that of the robust Gaussian regression filter. This is because the opening filter produces a rigorous lower envelope and thus the following watershed segmentation tends to generate larger contour areas. It is found the standard deviations of the parameter results of the morphological filter are larger than those of the robust Gaussian regression filter. This might attribute to the fact that the morphological filtration is determined by the local surface geometry and the ball. Therefore, the more complex the surface topography is, the more variation the filter will generate.

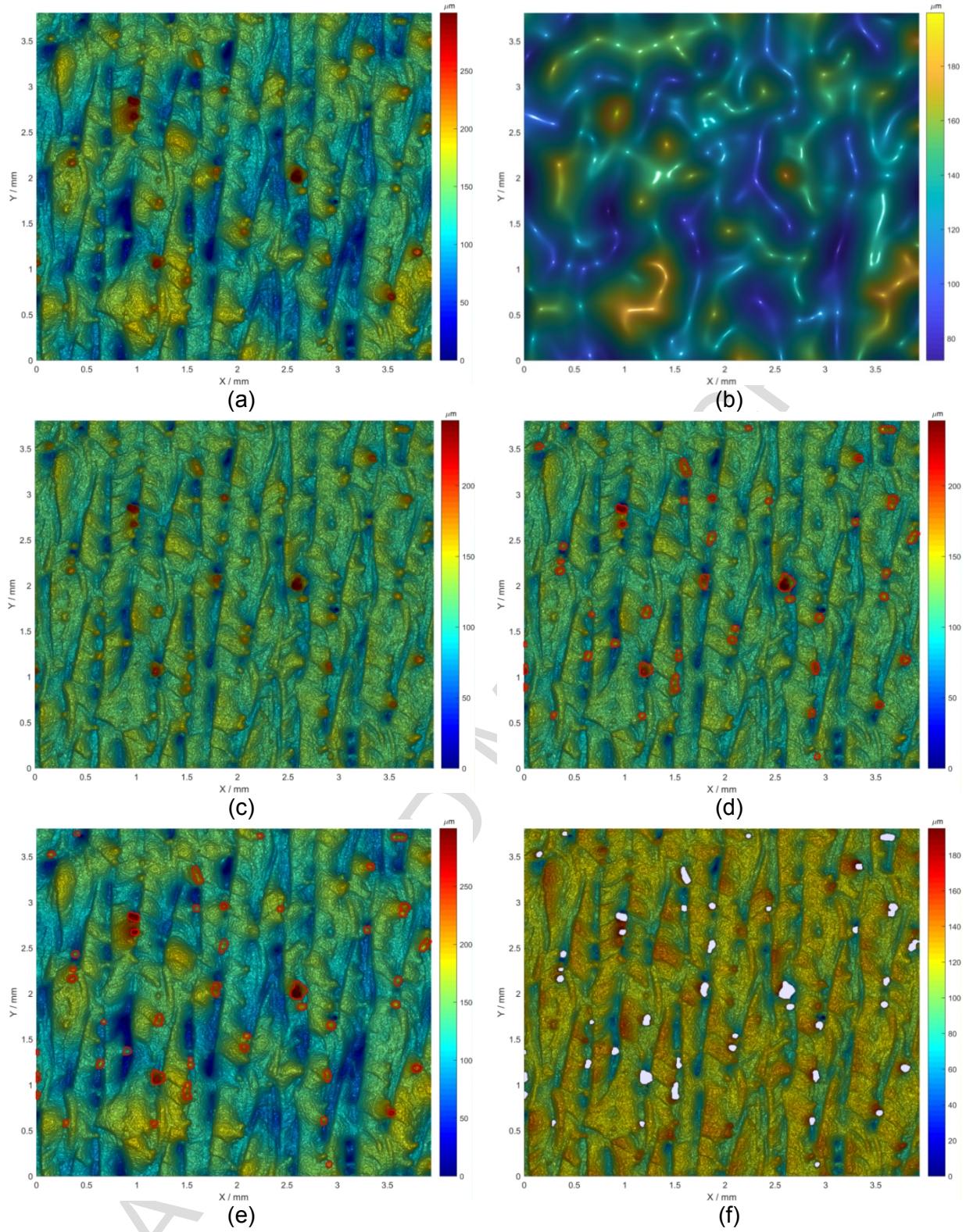

Figure 7. Extraction of the waviness surface and the globules of the measured EBM surface by applying the robust Gaussian regression filter and the watershed segmentation: (a) measured surface; (b) waviness surface; (c) residual surface; (d) residual surface with identified globules; (d) measured surface with identified globules; (e) underlying roughness surface with globules excluded.

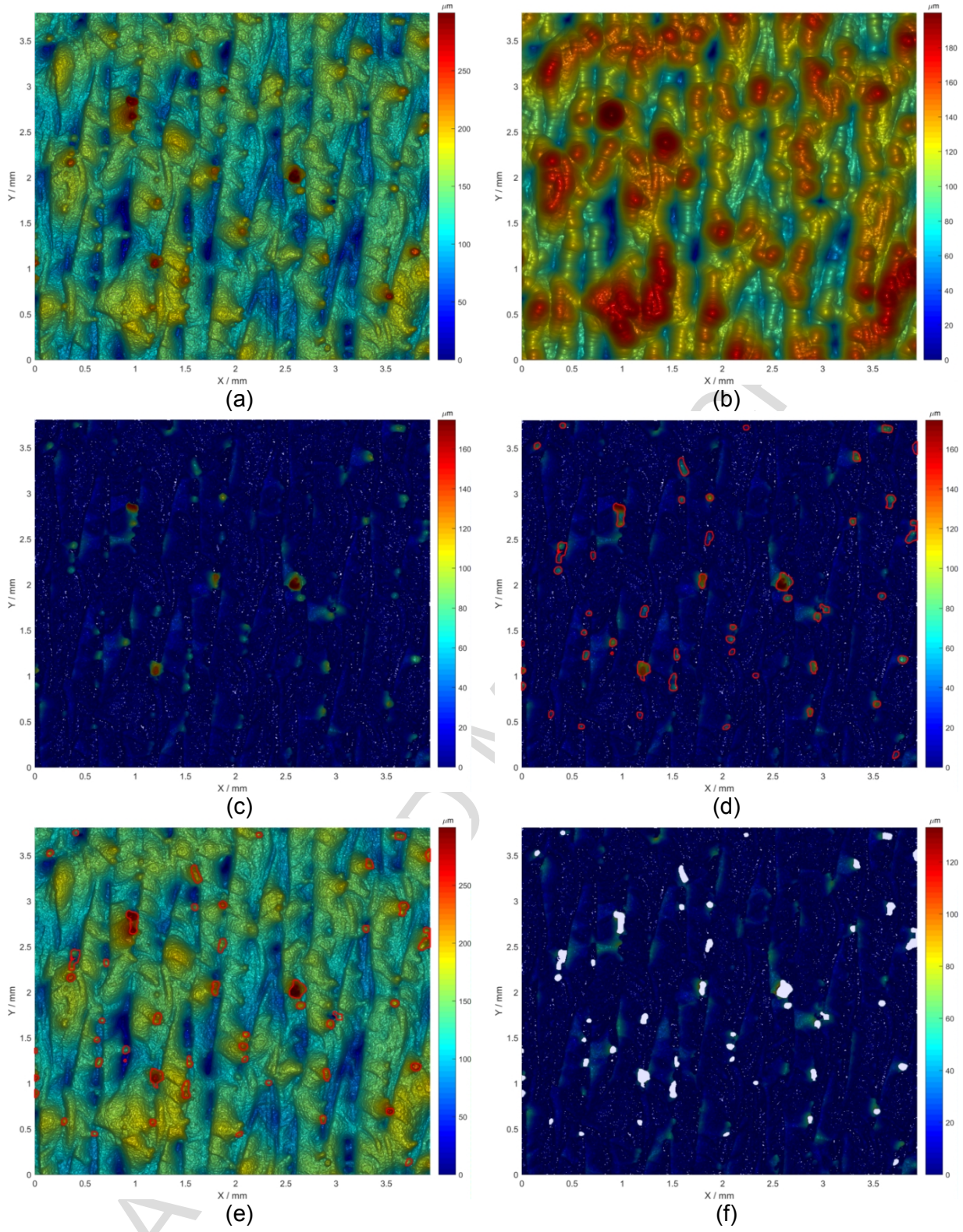

Figure 8. Extraction of the waviness surface and the globules of the measured EBM surface by applying the morphological opening filter and the watershed segmentation: (a) measured surface; (b) waviness surface; (c) residual surface; (d) residual surface with identified globules; (d) measured surface with identified globules; (e) underlying roughness surface with globules excluded.

Table 2. Results of selected surface texture parameters of different surface wavelength components of the measured EBM surface (the robust Gaussian regression filter and the watershed segmentation are applied).

Parameters	Waviness surface		Residual surface		Roughness surface	
	Mean values	STD	Mean values	STD	Mean values	STD
Sa / µm	16.49	1.26	11.7	0.4	11.28	0.33
Sq / µm	20.74	1.47	16.4	0.8	14.87	0.47
Ssk	-	-	-0.01	0.29	-0.68	0.20
Sku	-	-	7.43	1.29	4.96	0.60

Table 3. Results of globule parameters of the measured EBM surface (the robust Gaussian regression filter and the watershed segmentation are applied).

Total globule areas (mm^2)		globule area percentage to the whole surface		Total globule volume (mm^3)	
Mean values	STD	Mean values	STD	Mean values	STD
0.266	0.100	1.8%	0.7%	0.016	0.003

Table 4. Results of selected surface texture parameters of different surface wavelength components of the measured EBM surface (the morphological opening filter and the watershed segmentation are applied).

Parameters	Waviness surface		Residual surface		Roughness surface	
	Mean values	STD	Mean values	STD	Mean values	STD
Sa / µm	22.62	1.40	9.32	0.79	7.45	0.57
Sq / µm	28.46	1.71	14.64	1.51	10.71	0.73
Ssk	-	-	3.72	0.38	2.52	0.10
Sku	-	-	24.11	4.40	10.82	0.94

Table 5. Results of globule parameters of the measured EBM surface (the morphological opening filter and the watershed segmentation are applied).

Total globule areas / mm^2		globule area percentage to the whole surface		Total globule volume / mm^3	
Mean values	STD	Mean values	STD	Mean values	STD
0.289	0.062	1.9%	0.4%	0.024	0.004

5.2 SLM surfaces

Another group of measurements was performed on an SLM surface using the same measurement instrument. The SLM surface was measured using the configuration: 20x objective lens, ring light, vertical resolution 0.67 μm, lateral resolution 2.93 μm, sampling distance 3.92 μm (after data decimation) and 3x4 stitching. The measured SLM surface is 1.91 mm x 1.95 mm in size and presents finer surface texture in comparison to the EBM surface, due to the higher resolution of the SLM machine and finer material powders.

Figure 9 and 10 illustrate the application of the proposed characterisation procedures on the measured SLM surface. The λ_c and λ_f cut-off wavelengths are set to 0.08 mm and 1.5 mm respectively for the robust Gaussian regression filter, and the ball radius is set to 0.08 mm for the opening filter. The height thresholds are set to 45 μm and 20 μm for the following watershed segmentation for these two cases respectively. The results of surface texture parameters and globule parameters are listed in Table 6-9. In the case that the robust Gaussian regression filter and the watershed segmentation are used, the Sa and Sq of the underlying roughness surface is 6.4% and 11.5% less than those of the residual surface. Ssk changing from a positive value to a negative value after excluding the globules means the surface texture changes from a peak dominant case to a valley dominant case. The Sku value also has a decrease after the exclusion of the globules, which indicates that the globules on the SLM surface have large influence on surface height distribution. The results of the selected surface texture parameters and globule parameters produced by the morphological opening filter and the watershed segmentation show a similar pattern, see Tables 8 and 9.

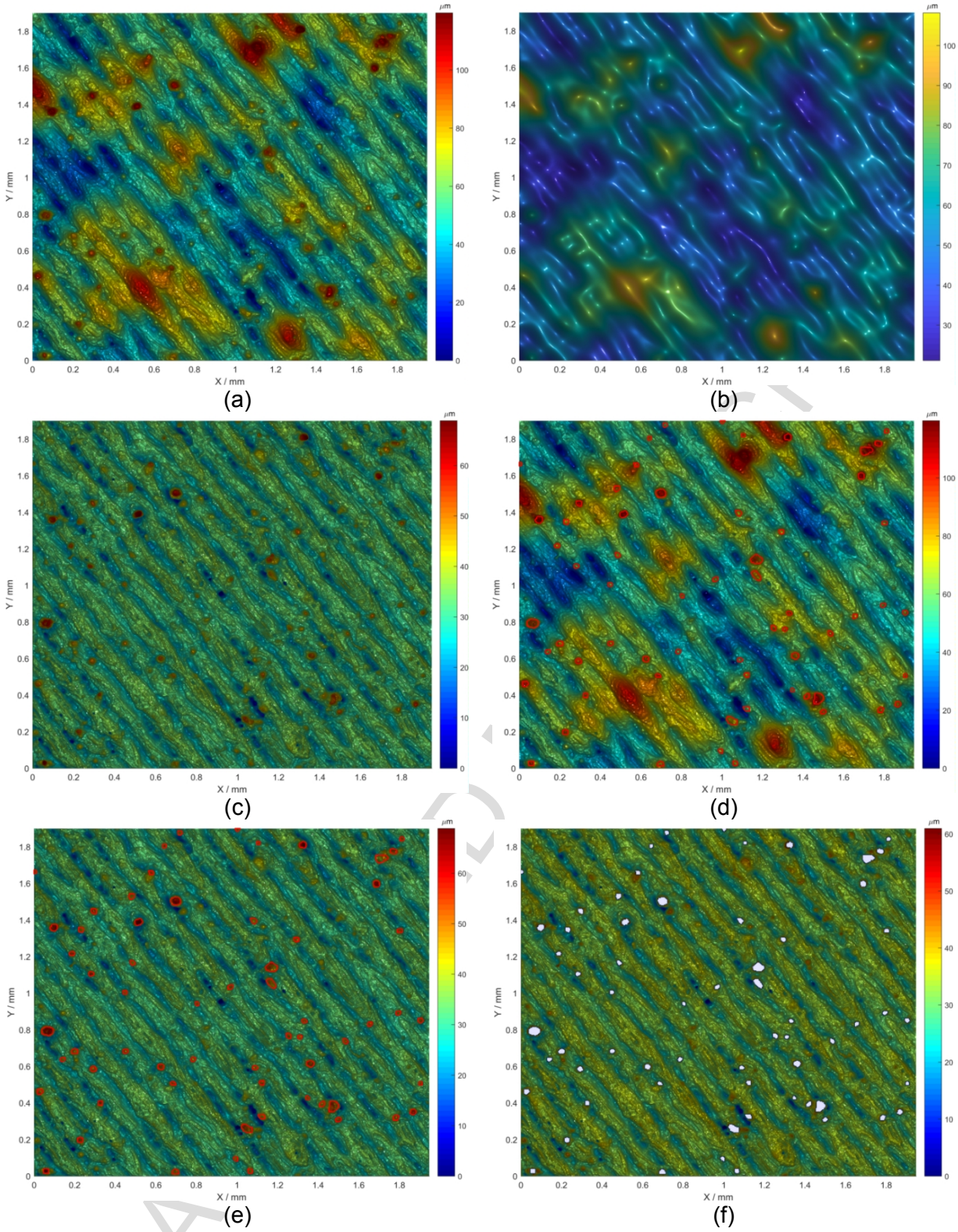

Figure 9. Extraction of the waviness surface and the globules of the measured SLM surface by applying the robust Gaussian regression filter and the watershed segmentation: (a) measured surface; (b) waviness surface; (c) residual surface; (d) residual surface with identified globules; (d) measured surface with identified globules; (e) underlying roughness surface with globules excluded.

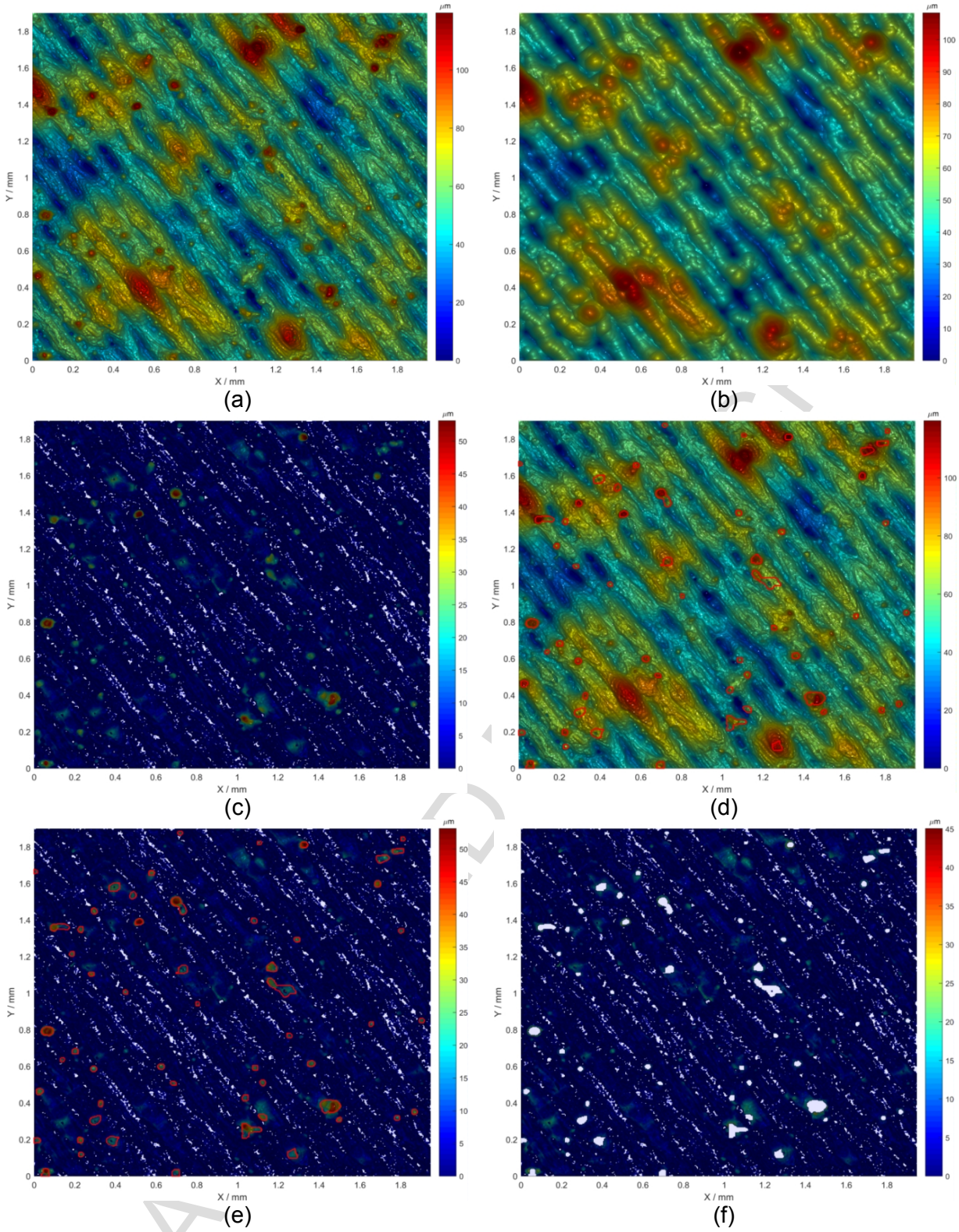

Figure 10. Extraction of the waviness surface and the globules of the measured SLM surface by applying the morphological opening filter and the watershed segmentation: (a) measured surface; (b) waviness surface; (c) residual surface; (d) residual surface with identified globules; (d) measured surface with identified globules; (e) underlying roughness surface with globules excluded.

Table 6. Results of selected surface texture parameters of different surface wavelength components of the measured SLM surface (the robust Gaussian regression filter and the watershed segmentation are applied).

Parameters	Waviness surface		Residual surface		Roughness surface	
	Mean values	STD	Mean values	STD	Mean values	STD
Sa / µm	10.69	0.63	3.26	0.04	3.05	0.04
Sq / µm	13.50	0.62	4.59	0.06	4.09	0.06
Ssk	-	-	0.12	0.06	-1.17	0.09
Sku	-	-	8.11	0.37	6.01	0.20

Table 7. Results of globule parameters of the measured SLM surface (the robust Gaussian regression filter and the watershed segmentation are applied).

Total globule areas / mm^2		globule area percentage to the whole surface		Total globule volume / mm^3	
Mean values	STD	Mean values	STD	Mean values	STD
0.066	0.014	1.8%	0.4%	0.001	0.000

Table 8. Results of selected surface texture parameters of different surface wavelength components of the measured SLM surface (the morphological opening filter and the watershed segmentation are applied).

Parameters	Waviness surface		Residual surface		Roughness surface	
	Mean values	STD	Mean values	STD	Mean values	STD
Sa / µm	11.04	0.74	2.48	0.08	2.05	0.10
Sq / µm	13.9	0.90	4.44	0.16	2.87	0.14
Ssk	-	-	4.61	0.27	2.65	0.11
Sku	-	-	32.51	3.21	17.51	1.93

Table 9. Results of globule parameters of the measured SLM surface (the morphological opening filter and the watershed segmentation are applied).

Total globule areas / mm^2		globule area percentage to the whole surface		Total globule volume / mm^3	
Mean values	STD	Mean values	STD	Mean values	STD
0.087	0.009	2.6%	0.2%	0.002	0.000

5.3 Discussion

The proposed surface characterisation methods enable the extraction of signature features of PBF processes. The characterisation of these signature features can facilitate building a better link between AM surface topography and AM process in comparison to conventional characterisation routes.

The robust Gaussian regression filter and the morphological filters are both qualified for the proper extraction of melted tracks, there needs further investigation before a judgement can be made on which filter is better for AM process control. Also, the use of a specific cut-off wavelength for the robust Gaussian does not implies using the same value of ball radius for the morphological filter. However, for a specified wavelength, an effective cut-off wavelength can be estimated by the ball radius [50]. The watershed segmentation can enable the extraction of globules. Even though it is noticed that some of the less significant globules are not identified, the algorithmic method is preferred in comparison to visual manual inspection due to the automated identification of globules as well as better repeatability and reproducibility. Obviously, the errors associated with the characterisation techniques need to be investigated. However, it is difficult for the PBF processes to produce a precise reference artefact to which extracted features can be compared. There also needs more investigation on how to determine a height threshold used for globule extraction, which should be more reliable to ensure the generation of more accurate segmentation results. It also worth comparing with other valid extraction methods [20, 21] for verification. A set of bespoke parameters are intentionally developed with the aim to offer a quantitative evaluation of the globules. Characterising different topographical features separately allows a more accurate control of AM process variables. The future work is to explore how to use these parameters to control relevant AM process variables.

Two types of filtration techniques are available for the extraction of melted tracks, i.e. the robust Gaussian regression filter and the morphological opening filter. More options are available for morphological filtration, such as the closing filter and the alternating sequential filters. The selection of the specific filtration technique is application dependent. For instance, the morphological method can be a good choice for the tribology related applications. Therefore, without referring to the specific application, the direction comparison of the robust Gaussian regression filter and the morphological filters does not make too much sense. However, the enriched toolbox can offer users more flexibility. The choosing of desired characterisation techniques is also affected by the specific AM surface topography. As mentioned in Section 3.1, there are cases that melted tracks are insignificant and globules take a dominant role, where the segmentation can be applied without using filtration in prior.

6. Conclusion

AM processes are different from traditional manufacturing process in nature, thus the topography of AM produced surface differs from those produced by traditional manufacturing. The characterisation of AM surface topography should take this critical fact into consideration. A state-of-the-art summary of surface characterisation of AM components has been conducted. It is noticed that the majority of published work follows the traditional surface characterisation routes without giving special consideration on the unique characteristics of PBF processes. To better link PBF surface topography with its process, an update of the surface characterisation framework is proposed. The description of surface spatial wavelength components and other significant PBF signature features along with their production mechanism are presented. Based on the updated framework, a bespoke characterisation procedure is developed for the extraction of various topographical features of PBF surfaces. The robust Gaussian regression filter and the morphological filters are used for the separation of waviness component and the enhanced watershed segmentation is employed for the extraction of globules and surface pores. These characterisation techniques are discussed in details with an emphasis on their relevance to PBF surface characterisation. Finally, two case studies are given, where two groups of measurements were taken from two EBM and SLM surfaces. The application of the proposed characterisation techniques was illustrated and compared.

Acknowledgement

Dr S Lou would like to thank Prof T Iain & Dr H Martin from the University of Sheffield and Dr M Antar & Dr TL See from the Manufacturing Technology Centre for supplying AM samples. The authors would like to thank Dr A Yacoot, Dr D O'Connor and Dr A Lewis, for assistance with proofreading. From NPL, Dr Sun W gratefully acknowledges the National Measurement System Programme for Engineering & Flow metrology for funding this work. From the University of Huddersfield, the authors gratefully acknowledge the UK's Engineering and Physical Sciences Research Council (EPSRC) funding of the Future Advanced Metrology Hub (EP/P006930/1). Dr S Lou gratefully acknowledges the Researcher in Residence scheme (EP/R513520/1) for supporting this work.

References

[1] TSB Additive Manufacturing Special Interest Group. Shaping our national competency in additive manufacturing: a technology innovation needs analysis, 2012.
[2] Berman B. 3-D printing: the new industrial revolution, Bus Horiz 2012;55: 155-162.
[3] National Institute of Standards and Technology. Measurement science roadmap for metal-based additive manufacturing, https://www.nist.gov/sites/default/files/documents/el/isd/NISTAdd_Mfg_Report_FINAL-2.pdf, 2013 [accessed on 12 Jan 2018].
[4] Gibson I, Rosen DW, Stucker B. Additive manufacturing technologies: rapid prototyping to direct digital manufacturing. New York, USA: Springer; 2015. p.138.
[5] Kruth JP, Yasa E, Deckers J. Roughness improvement in selective laser melting. Proc. of Int. Conf. PMI, Ghent, Belgium, 2008: 170-183.
[6] Dalgarno K. Materials research to support high performance RM parts. Rapid manufacturing 2nd international conference, 2007: 147-56.
[7] Mumtaz K, Hopkinson N. Top surface and side roughness of Inconel 625 parts processed using selective laser melting. Rapid Prototyp J 2009;15(2): 96-103.
[8] Strano G, Hao L, Everson RM, Evans KE. Surface roughness analysis, modelling and prediction in selective laser melting. J Mater Process Technol 2013;213: 589–597
[9] Ghanekar A, Crawford R. Optimization of SLS process parameters using D-optimality. Proc. 14th Int. Solid Freeform Fabrication Symp 2003: 348-62.
[10] Bacchewar PB, Singhal SK, Pandey PM. Statistical modelling and optimization of surface roughness in the selective laser sintering process. Proc Inst Mech Eng B: J Eng Manuf 2007;221: 35-52.
[11] Yadroitsev I, Gusarov A, Yadroitsava I, Smurov I. Single track formation in selective laser melting of metal powders. J Mater Process Technol 2010;210: 1624-1631
[12] Triantaphyllou A, Giusca GL, Macaulay GD, Roerig F, Hoebel M, Leach RK, Tomita B, Milne KA. Surface texture measurement for additive manufacturing. Surf. Topogr.: Metrol. Prop, 2015;3: 024002.
[13] Karlsson J, Snis A, Engqvist H, Lausmaa J. Characterization and comparison of materials produced by electron beam melting (EBM) of two different Ti-6AL-4V powder fraction. J Mater Process Technol 2013;213: 2109-2118.
[14] Fox JC, Moylan SP, Lane BM, Whitenton BM, Heigel JC. Preliminary study toward surface texture as a process signature in laser powder bed fusion additive manufacturing. Proc ASPE Summer Topical, 2016.
[15] Cooper DE, Stanford M, Kibble KA, Gibbons GJ. Additive manufacturing for product improvement at Red Bull Technology. Mater & Des 2012;41: 226-230.
[16] Whitehouse D. Surfaces and Their Measurement, Hermes Penton Science, 2002.
[17] Grimm T, Wiora T, Witt G. Characterization of typical surface effects in additive manufacturing with confocal microscopy, Surf Topogr: Metrol Prop, 2015;3: 014001.
[18] Vetterli M, Schmid M, Wegener K. Comprehensive investigation of surface characterization methods for laser sintered parts. Fraunhofer Direct Digital Manufacturing Conference, 2014.

[19] Reese CZ, Taylor JS, Evans CJ. Surface finish metrology of additive-manufactured components. Proc ASPE Summer Topical 2016: 50-54.
[20] ISO 25178-2 Geometrical product specifications (GPS) -- Surface texture: Areal -- Part 2: Terms, definitions and surface texture parameters, 2012.
[21] Senin N, Thompson A, Leach RK Feature-based characterisation of signature topography in laser powder bed fusion of metals, Meas Sci Technol 2018 29(4).
[22] Lou S, Townsend A, Blunt L, Zeng W, Jiang X, Scott JP. On characterising surface topography of metal powder bed fusion additive manufactured parts. Proc. 16th EUSPEN, 2016.
[23] Rosa B, Brient A, Samper S, Hascoët JY. Influence of additive laser manufacturing parameters on surface using density of partially melted particles, Surf Topogr: Metrol Prop 2016;4: 045002.
[24] ISO 4287 Geometrical Product Specifications (GPS) -- Surface texture: Profile method -- Terms, definitions and surface texture parameters, 1997.
[25] Sidambe AT. Three dimensional surface topography characterization of the electron beam melted Ti6Al4V. Met Powder Rep, 2017; 72: 200-205.
[26] Lemoine AC, Mancini MP, Velez JA, Brown CA. On the metrology of surface produced by laser melting of powders. Proc ASPE Summer Topical 2016: 174-179.
[27] Pagani L, Qi Q, Jiang X, Scott PJ. Towards a new definition of areal surface texture parameters on freeform surface, Measurement 2017;109: 281-291.
[28] Jiang XJ, Whitehouse DJ, Technological Shifts in Surface Metrology, CIRP Ann Manuf Technol, 61 (2) (2012), pp. 815–836.
[29] Thompson A, Senin N, Leach R. Towards an Additive Surface Atlas, Proc ASPE Summer Topical, 2016.
[30] Niu HJ, Chang TH. Instability of scan tracks of selective laser sintering of high speed steel powder. Scripta Mater 1999;41: 1229-1234.
[31] Simonelli M, Tuck C, Aboulkhair NT, Maskery I, Ashcroft I, Wildman RD, et al. A study on the laser spatter and the oxidation reactions during selective laser melting of 316L stainless steel, Al-Si10-Mg, and Ti-6Al-4V. Metall Mater Trans A 2015;46: 3842-3851.
[32] Thijs L, Verhaeghe F, Craeghs T, Humbeeck JV, Kruth JP. A study of the microstructural evolution during selective laser melting of Ti–6Al–4V. Acta Mater. 2010;58: 3303–3312.
[33] Tammas-Williams S, Zhao H, Léonard F, Derguti F, Todd I, Prangnell PB XCT analysis of the influence of melt strategies on defect population in Ti–6Al–4V components manufactured by selective electron beammelting. Mater Charact 2015;102: 47-61.
[34] ISO 25178-3 Geometrical product specifications (GPS) -- Surface texture: Areal -- Part 3: Specification operators, 2012.
[35] ISO 4287 Geometrical Product Specifications (GPS) -- Surface texture: Profile method -- Terms, definitions and surface texture parameters, 1997.
[36] Scott PJ. Foundation of decomposition for manufacturing geometrical products, the 16'th metrology and properties of engineering surfaces, Göteborg, Sweden, 2017.
[37] Zeng W, Jiang X, Scott PJ. Fast Algorithm of the Robust Gaussian Regression Filter for Areal Surface Analysis, Meas Sci Technol 2010:21: 055108.
[38] Lou S, Jiang X, Scott PJ. Geometric computation theory for morphological filtering on freeform surfaces, Proc R Soc London, Ser A, 2013;469: 20130150.
[39] Scott PJ. Pattern analysis and metrology: the extraction of stable features from observable measurements, Proc R Soc London, Ser A 2004;460: 2845-2864.
[40] ISO 16610-30 Geometrical product specifications (GPS) -- Filtration -- Part 30: Robust profile filters: Basic concepts, 2015.
[41] Seewig J. Linear and robust Gaussian regression filters. J Phys: Conf Ser, 2005;13: 254–257.
[42] Jiang X. Robust solution for the evaluation of stratified functional surface CIRP Ann. Manuf. Technol. 2010; 59 573-76
[43] ISO 16610-40 Geometrical product specifications (GPS) -- Filtration -- Part 40: Morphological profile filters: Basic concepts, 2015.
[44] Malburg CM. Surface profile analysis for conformable interfaces J. Manuf. Sci. Eng., Trans. ASME 2003;125: 624–27

[45] Lou S, Jiang X, Scott PJ. Correlating motif analysis and morphological filters for surface texture analysis, Measurement, 2013;42: 993-1001.
[46] Lou S, Jiang X, Bills P, Scott PJ. Defining true tribological contact through application of the morphological method to surface topography. Tribol. Lett., 2013;50: 185-193.
[47] Serra J., Vincent L. An overview of morphological filtering. Circ. Syst. Signal Pr., 1992;11: 47-108.
[48] Scott PJ. Feature parameters. Wear 2009;266: 548-551.
[49] Gonzalez RC, Woods RE, Eddins SL Digital image processing using MATLAB, Prentice Hall, 2003.
[50] Leach R., Haitjema, H. Bandwidth characteristics and comparisons of surface texture measuring instruments. Meas Sci Technol, 2010;21(3): 032001

Highlights

- A state-of-the-art review of the AM surface texture characterisation is provided.
- Significant topographical features of PBF layer surfaces are identified and described.
- A bespoke surface characterisation procedure is developed for PBF surface texture.
- The developed characterisation techniques are applied to two SLM and EBM surfaces.